Effect of Chloride and Sulphate Environments on the Compressive Strength, Density and Electrical Resistivity of Ultra-High Performance Concrete (UHPC)

Samaneh Khaksefidi[1], Mansour Ghalehnovi[2*], Jorge de Brito[3], HosseinAli Rahdar[1]

1. Assistant Professor, Department of Civil Engineering, University of Zabol, Zabol, Iran
2. Professor, Department of Civil Engineering, Ferdowsi University of Mashhad, Mashhad, Iran
3. Professor, CERIS, Department of Civil Engineering, Architecture and Georresources, Instituto Superior Técnico, Universidade de Lisboa, Lisbon, Portugal

Corresponding author: Ghalehnovi@ferdowsi.um.ac.ir

ARTICLE INFO

ABSTRACT

Concrete resistance to chloride ion penetration is an important parameter against the corrosion of rebars. The rapid chloride permeability test has already been used to predict UHPC's resistance at ages up to 28 days under different curing regimes. However, the simple and non-destructive surface electrical resistivity (ER) method, standard specimens, for longer than 28 days and the effects of sulphate and chloride have seldom been considered in UHPC. Here, the ER and compressive strength (CS) tests were performed on 45 UHPC cylindrical specimen with a diameter of 10 cm and a height of 20 cm cured in water, 10% magnesium sulphate and 3.5% sodium chloride solutions for 7, 14, 28, 56 and 90 days. The ER, CS and density increase with age. However, concerning the reduction in ER, the chloride environment was more damaging than the sulphate one. In addition, sulphate had a more destructive effect than chloride on the 90-day CS, so that 3.5% sodium chloride and 10% magnesium sulphate solutions resulted in a decrease after 90 days of 8.73% and 25.5% compared to the control sample, respectively. Furthermore, the curing process affected density's evolution. Chloride ion penetration was negligible in the specimens cured in water and very low in those cured in the sodium chloride and magnesium sulphate solutions. The results were interpreted by XRD, EDS and SEM. A correlation between ER and CS is proposed.

1. Introduction

Significant annual costs ensue from repairing concrete structures such as docks and bridge piers in corrosive environments. Many studies have proposed various methods and additives to reduce the detrimental effects of corrosive environments and improve the quality of concrete [39, 49]. These methods make use of Type II and V Portland cement, cement substitutes such as synthetic pozzolans including fly ash, micro silica, nano-clay, rice husk ash (RHA), smelting furnace slag, and natural pozzolans such as ash, pumice, and volcanic tuffs [27, 19, 23]. UHPC is known as concrete with high compressive strength, high density, low permeability and high durability. The concept of performance has always been a subject of controversy among researchers because of its wide scope [35]. There are studies that examined the properties of UHPC under different conditions. Yazici et al. [48] concluded autoclave curing is more effective than conventional curing in terms of increasing the compressive strength of concrete. However, the optimisation of autoclave curing concerning the mechanical properties of samples depends on the optimum curing temperature, pressure and time. Saeidiyan and Madhkhan [38] further investigated the durability of UHPC reinforced with glass fibre under melting and ice cycles under both conventional and autoclave curing conditions. They reported that autoclave curing increased the

compressive strength in fibre-free samples by about 20% compared to conventional curing; however, it did not have any significant effect on the compressive strength of samples with fibres. By adding sodium chloride at 0 to 3 wt% of cement to concrete, Pyo et al. [31] studied the effect of sodium chloride on the visual appearance, changes in electrical resistivity, flexural strength, compressive strength, and Young's modulus of UHPC. Madani and Pourjhanshahi [24] showed that silica fume as a pozzolan substitute for cement had a positive effect on the durability of UHPC, and wet curing at 60 ºC was suitable for accelerated curing. Shen et al. [40] showed that, by increasing the curing temperature from 20 ºC to 250 °C, the mechanical properties of UHPC improved due to the formation of additional hydrates, improvement in the transition zone around the steel and quartz fibres, and increase in the average chain length of the hydrates and pozzolanic reactions between silica fume, quartz and calcium hydroxide.

1.1. Importance of electrical resistivity

Chloride ions penetration is the most important factor in the corrosion of reinforcing bars (rebars) in concrete. In the corrosion process on the rebar's surface, there are two anodic and cathodic zones with potential differences (Figure 1). The transport of hydroxide ions from cathode to anode is influenced by the specific electrical resistivity of concrete [22].
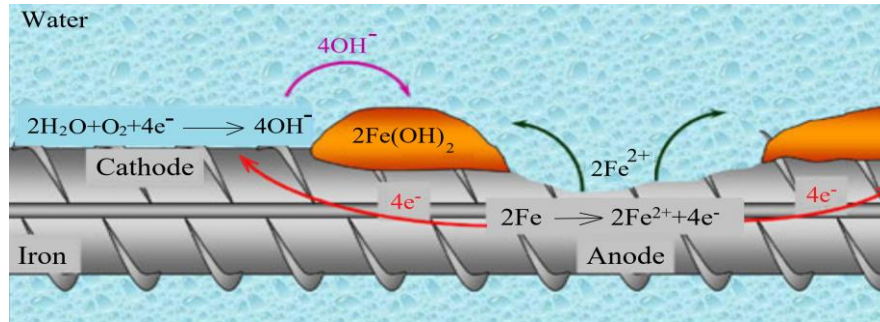
Figure 1. Schematic representation of the corrosion process of the rebar [43]

RCPT (Rapid Chloride Permeability Test) is a common experiment carried out in a relatively short time to evaluate concrete resistance to chloride ion penetration. However, it is relatively difficult and expensive, requiring special equipment. Despite the nature drawbacks of the test, it is still used owing to its longevity and the availability of the results pertaining to many different concrete samples at different ages. Another method is the measurement of the electrical resistivity (ER) of concrete. Major efforts have been made to correlate the results of these tests. Table 1 presents a general comparison of these test results and concrete resistance to chloride ion penetration according to the relevant standards. Therefore, ER can be used to determine the concrete resistance to penetration of chloride ions and the probability of rebar corrosion in concrete. Some studies have reported a correlation between ER and the processes of initiation and expansion in corrosion. Table 2 presents criteria to evaluate corrosion activity in terms of concrete's ER according to several researches [17]. In general, the conductivity of concrete depends on both the microstructure of capillary pores and the pore fluid's conductivity. The ER of concrete indicates the movement of ions such as chloride ions, in the pore structure of concrete. Accordingly, the ER of a material is defined as its ability to resist the charge transfer [17].

Table 1: Relationship between electrical resistivity and chloride ion penetration [1-3]

Chloride ion penetration	Charge passed in RCPT (Coulomb)	Surface resistivity test 100-by-200-mm cylinder (kΩ-cm) (a=3.81 cm)	Bulk resistivity (kΩ cm)
High	4000>	12<	6.3<
Moderate	4000–2000	21–12	11–6.3
Low	2000–1000	37–21	20–11
Very low	1000–100	254–37	134–20
Negligible	100<	254>	134>

a = Wenner probe tip spacing

Table 2: Criteria to evaluate corrosion in terms of electrical resistivity [17]

References	Evaluation of corrosion in terms of electrical resistivity (Ω.m)		
	High	**Moderate**	**Low**
Cavalier and Vassie 1981	50<	50–120	120>
Hope et al. 1985	65<	65–85	85>
Lopez and Gonzalez 1993	70<	70–300	300–400 >
Morris et al. 2002	100<	100–300	300>
Gonzalez et al. 2004	200<	200–300	1000>
Elkey and Sellevold 1995	50<	Under discussion	100 –730>
Andrade and Alonso 1996	100<	100–1000	1000 –2000>
Polder et al. 2001	100<	100–1000	1000>
Broomfield and Millard 2002	50<	50–200	200>
Smith et al. 2004	80<	80–120	120>

According to Spragg et al. [42], factors such as sample geometry, saturation degree, test temperature, curing conditions, presence or absence of rebars, measurement method, electrode distance, measurement position in the surface method, and sample age affect the results of the ER test. The saturation degree is the most important factor affecting the ER of concrete [17]. According to the Büyüköztürk and Taşdemir's [12] larger volume and size of aggregates increases the ER. Azarsa and Gupta [11] reviewed the role of electrical resistivity in evaluating concrete durability in various references. Their article further addressed the researchers' concerns about parameters affecting the measurement of electrical resistivity, such as the environmental conditions and the existence of rebars and cracks in concrete. They also described common techniques to measure the ER of concrete, there are several methods vary in terms of the type of applied current (alternating and direct) and the configuration of the applied electrodes. According to Polder [30], ER in concrete should be measured by an alternating current. The use of direct current is not recommended due to the inductive effect of electrode polarization that leads to major errors.

The review of the literature reveals that most of the researches have been conducted on UHPC specimens exposed to steam, autoclaving, and high temperatures, or added additions to concrete. However, little on UHPC is available on sulphate and chloride degradation [13]. The present study investigated characteristics of UHPC such as compressive strength, density and chloride ion penetration through the determination of electrical resistivity, under sulphate and chloride curing conditions. Moreover, the correlation between compressive strength and electrical resistivity is not the same for

different cementitious materials, since it depends on their microstructure. Therefore, although the correlation equations between electrical resistivity and compressive strength were proposed for different concrete mixes, so far there is no proposed equation for UHPC. Therefore, this study also intends to propose a suitable correlation equation between electrical resistivity and compressive strength for UHPC. By providing an appropriate relationship between ER and CS and measuring non-destructive ER, which is an easy procedure, an estimate can be obtained of the compressive strength of in-service concrete structures. This becomes more important when there is no information regarding concrete's design strength or corrosive condition effect, and concrete coring is impossible. The concrete microstructure and further interpretations of results were then examined with the help of X-ray diffraction experiment and electron microscopy images. Also, although several researchers have studied on chloride ion penetrability of UHPC, very limited studies used the simple and non-destructive surface electrical resistivity method on standard specimens. In addition, these studies were carried out mostly at ages up to 28 days and long-term exposure studies are very scarce. Therefore, this study investigated the specifications of UHPC specimens at 7, 14, 28, 56 and 90 days of age and used the four-point Wenner method with alternating current to measure ER from the surface. A further description of this method is provided in the following sections.

2. Experimental program

2.1. Materials and mix design

The UHPC produced in this study is normal UHPC without fibres, made from local materials commercially available in Iran and cured in ambient laboratory temperature. The material properties are as follows: Type II Portland cement with chemical composition according Table 3 , micro silica with an average diameter of 0.1 micron [8] and with a specific weight of 2.50 g/cm, quartz powder with a particle diameter lower than 10 micrometres, silica sand with a specific weight of 2.33 g/cm^3, superplasticizer and water. Superplasticizer is used to reduce water consumption, increase efficiency, strength, slump, and lubrication, reinforce the water tightness of concrete, and achieve quality and durability in the hardened concrete. A carboxylate-based superplasticizer is recommended either in concrete with standard requirements to minimize the water/cement ratio, or in specialized concrete with minimum W/C ratios and maximum durability [7, 9, 6]. Polycarboxylic ethers have a comb-like structure. The structure of this superplasticizer is presented in Figure 2 [4]. Here, a normal carboxylate-based plasticizer was used with the commercial name of Sure Plast 402, which is a honey-coloured liquid with a specific weight of 1.01 ± 0.02 g/cm^3 at 25 °C.

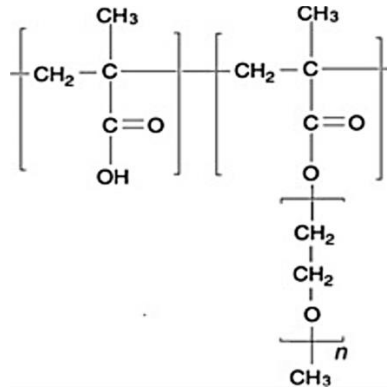The mix design was selected according to the studies of Rahdar and Ghalehnovi [34], as presented in Table 4.

Figure 2. Chemical structure of polycarboxylic ethers [4]

Table 3: Chemical composition of cement [18]

Composition	SiO_2	Al_2O_3	Fe_2O_3	CaO	MgO	SO_3	Na_2O	K_2O	L.O.I.	C_3S	C_2S	C_3A	C_4AF	I.R.
Content (%)	21.00	4.60	3.90	62.5	2.90	2.00	0.5	0.45	1.40	54	23	5.60	12	0.3

Table 4: UHPC mix proportions [34]

Materials	Type II Portland cement	Micro silica	Quartz silica powder	Silica sand	S.P.(3%)	Water
Content (kg/m³)	680	200	285	1020	20.1	178

2.2. Preparation of samples

First, all materials were weighted and half of the superplasticizer was mixed with water. Dry materials were then mixed for 2 minutes, and a part of water and superplasticizer was slowly added to the mix over a 2-minute period, as mixing proceeded. [20, 21]. After one minute, the remaining superplasticizer and water were added to the mix for 30 seconds. The mixing process lasted about 2 to 3 minutes until the dry powder mix turned into mortar [33]. It was then poured into cylindrical moulds of 10 cm in diameter and 20 cm in height within 15 minutes (Figure 3). To retain moisture, the samples were covered with plastic for up to 24 hours; next, the samples were removed from the mould, kept in water for a day and transferred to the curing solutions. The solutions were prepared by dissolving the required amount of desired salt in a given amount of drinking water. To control the concentration of the solution during curing, the water level in the container was controlled and the solution was stirred every day.

Figure 3.   Preparation of specimens

The study on the compressive strength, density and electrical resistivity of the samples was considered in the laboratory program agenda. Due to the destructive effect of chloride and sulphate environment on concrete, 10% magnesium sulphate and 3.5% sodium chloride solutions were considered as corrosive environments, with water considered as control. Five ages (7, 14, 28, 56 and 90 days) and three samples per age were considered to measure compressive strength. Owing to the non-destructive nature of the electrical resistivity and density tests, the same samples were used for these tests. Therefore, the present study prepared and examined 15 samples for each curing environment, amounting to 45 samples. The names of the samples were in accordance with the AB-I pattern.

First section (A): W stands for water, CL represents 3.5% sodium chloride solution and Mg 10% magnesium sulphate solution. Second section (B): the considered sample age for the compressive strength test. Third

section (C): sample number with similar conditions.

2.3. Determination of surface electrical resistivity of concrete using the Wenner Test

The test is performed non-destructively on a main structure or samples taken from fresh concrete. The Wenner test device has four electrodes with equal distances (a) located on a straight line on the surface of the samples (AASHTO, 2019). Figure 4 shows the sample during surface electrical resistivity test using a Wenner device.

As shown in Figure 4, the electrical current with a specified frequency (I) is provided by a current source between two external electrodes and voltage (V) is measured at two internal electrodes. The surface electrical resistivity of concrete is then calculated according to the following equation:

$$\rho = 2\pi a \frac{V}{I} \qquad (1)$$

Where ρ is the electrical resistivity (Ω.m), a is the distance between electrodes (m), V is
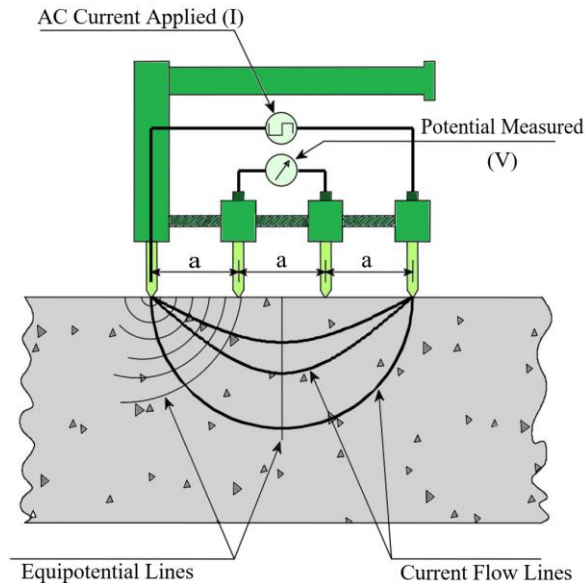
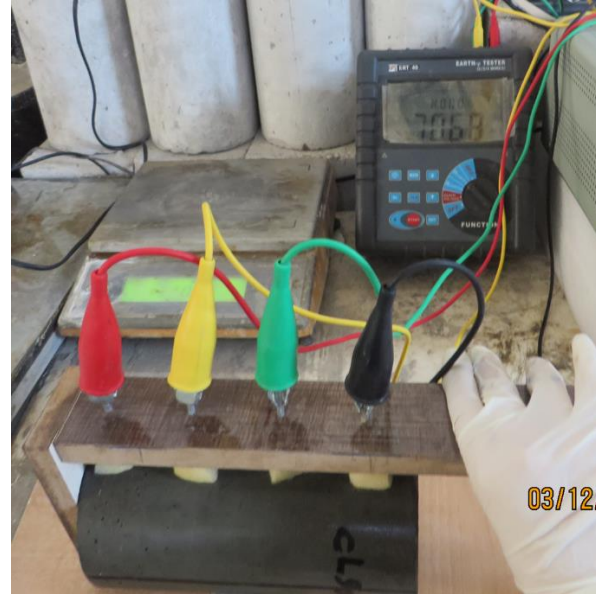the applied voltage (V) and I is the current intensity (A).

Figure 4. Four-Point Wenner Probe Test Setup [3]

According to the FDOT (Florida Department of Transportation) (FDOT, 2004) and AASHTO (AASHTO, 2014, AASHTO, 2019) standards, the test should be performed on 20×10 cm cylindrical samples. ER was read by inserting the electrodes along the sample's length and rotating twice around the circumference of the circle at angles of 0º, 90º, 180º and 270º. Surface electrical resistivity was reported as an average of eight readings. Due to the strong influence of sample saturation on this property, it was ensured that the samples were completely saturated and all specimens had equal surface moisture while reading. For this purpose, immediately after the specimen exited from the solution, the surface water was dried with a cloth and placed on a dry wooden support. The electrodes were 5 cm apart, and the test

was performed at the usual laboratory temperature.

2.4. Determination of compressive strength and density

The compressive strength and density of the specimens were measured at 7, 14, 28, 56 and 90 days. Compressive strength was specified according to ASTM C39 [10], using a 300-ton concrete compression machine. Furthermore, the weight of the samples was measured with a precision of 0.1 g in saturated surface dry conditions. Regardless of the changes in sample's size, density was calculated as the weight divided by the sample's volume.

3. Results and discussion

3.1. Effect of the curing conditions and sample age on compressive strength

Table 5 and Figure 5 show the average compressive strength *versus* sample's age for different curing conditions. Each column on the graph shows the mean compressive strength of three similar samples at a specified age. Standard error bars are also shown.

Table 5: Compressive strength

| Age (day)	Water			Sodium chloride solution			Magnesium sulphate solution		
	Average CS (MPa)	Standard deviation	Standard error	Average CS (MPa)	Standard deviation	Standard error	Average CS (MPa)	Standard deviation	Standard error
7	72.12	0.61	0.35	67.62	6.34	3.66	83.46	1.22	0.70
14	88.49	2.30	1.33	78.00	6.44	3.72	84.96	4.35	2.51
28	111.51	2.66	1.54	97.38	4.19	2.42	76.34	2.43	1.41
56	118.41	0.27	0.16	107.15	1.62	0.94	87.61	0.14	0.08
90	121.26	2.19	1.26	110.68	4.10	2.36	90.34	8.99	5.19
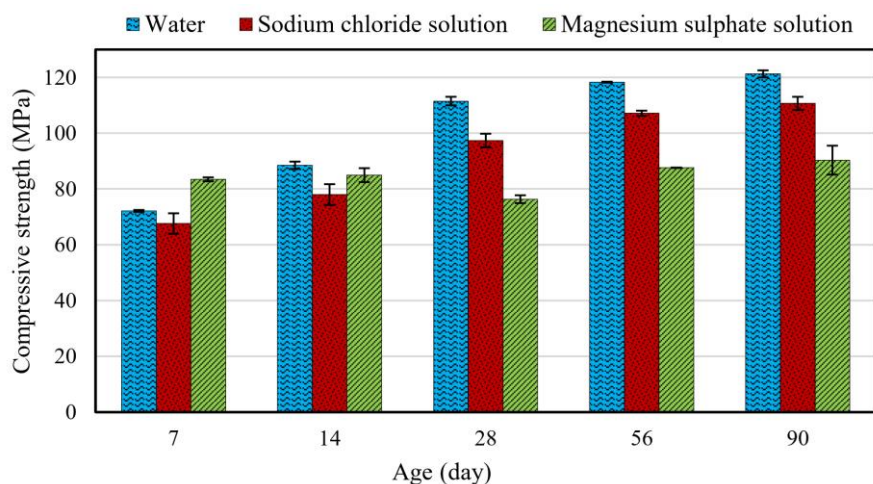
Figure 5. Average compressive strength of the specimens at all ages

Concrete strength increases over time because hydration reactions occur and products fill the original pores and make the concrete denser. The rate of strength increase is higher at early ages (about the 7 days) and after 56 days becomes almost constant. The greater increase in strength in the initial days can be attributed to the higher precipitation of hydration products in the samples. The main hydration product is calcium silicate hydrate (**C-S-H**), which mainly contributes to the strength gain of the samples [47]. Up to 28 days, the accumulated hydration products sharply increase. As curing time increases, the solid hydration products connect with each other. The formation of hydrated phases, such as **C-S-H**, is the main factor in this function. Afterwards, as the hydration reaction is almost complete, the strength level becomes quasi-constant. In

general, the increase in strength can be attributed to the higher precipitation of hydration products in samples during curing time. In this process, the voids and porosity may be randomly enclosed between the hydration products, which results in the material's discontinuity and weakness of the specimens and reduces the strength development rate. On the other hand, corrosive agents could disturb the hydration reactions and retard the development of concrete strength or damage the specimen's concrete structure. The graph shows that the sodium chloride environment decreased the compressive strength by 12.68%, 9.43% and 8.73% respectively, and the magnesium sulphate environment decreased the compressive strength by 31.54%, 25.94%, and 25.50%, respectively, compared to the control at 28, 56 and 90 days. The comparison of numbers at different ages for each corrosive environment showed that the differences from the control sample reduced by increasing the age from 28 to 90 days. It indicates that, due to the low permeability of UHPC, despite the corrosive agents concrete strength gain with age, and only its rate was reduced. On the other hand, in any environment, as age increased from 56 to 90 days, the rate of decrease in compressive strength was lower than that in the range of 28 to 56 days. Therefore, after 90 days' exposure of the specimens to corrosive environment curing, strength development retards and it will no longer be possible to obtain as much strength as in the control sample. Moreover, the longer exposure of samples to corrosive environment had more destructive effects on the compressive strength. Based on the compared reduction rate over a period of 28 to 90 days, the long-term exposure of magnesium sulphate solution decreased the compressive strength

more than the sodium chloride environment. It was also found by Zhao et al. [50, 51] and Mangi et al. [25]. It can be explained by this fact that external sulphate attack, in addition of physical damage due to crystallization of the sulphate salts, lead to chemical reactions with hydration products that generally produce corrosion products such as ettringite ($Ca_6Al_2(SO_4)_3$ $(OH)_{12} \cdot 26H_2O$) and gypsum (Calcium sulphate dehydrate, $CaSO_4 2H_2O$). Ettringite's increase within solid volume causes expansion by excessive filling of cracks and puts concrete under tension, which causes new cracks and extensions of the original cracks. Also gypsum can lead to softening and loss of cohesion between the hydration products which leads to gradual strength loss. On the other hand, when sulphate attack results from magnesium sulphate, in addition to ettringite and gypsum, brucite (Magnesium hydroxide, $Mg(OH)_2$) will be formed according to the following reaction:

$$MgSO_4 \quad + \quad Ca(OH)_2 \quad + \quad 2H_2O \quad \rightarrow$$

$$Mg(OH)_2 \quad + \quad CaSO_4 \quad \cdot \quad 2H_2$$

(2)
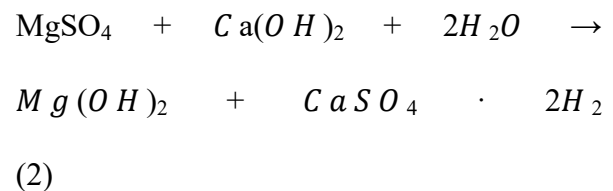
Magnesium sulphate will cause speedier degradation of the C-S-H phase. The consumption of calcium hydroxide, followed by the decalcification of the C-S-H phase in the hydration products to restore calcium hydroxide stability, will gradually cause loss of concrete strength. Even though formation of ettringite at long-term exposure is destructive, it may improve the compressive strength at short-time exposure due to filling the pores and reducing their sizes, consequently causing concrete to be denser. It can be observed in Figure 5 that curing in a

magnesium sulphate solution resulted in greater increase of compressive strength in the first week than the control specimen, as confirmed by Mangi et al. [25] and Zhao et al. [50, 51]

3.2. Effect of the curing conditions and sample age on surface electrical resistivity

Figures 6 to 8 show the diagrams of surface electrical resistivity's changes versus the sample age for different curing conditions and proposed equations. Previous researchers used different functions, such as power, hyperbolic and exponential equations, to calculate the relationship between the surface resistivity and curing age for different kind of concrete. Here, a quadratic function is proposed for each of the three environments.
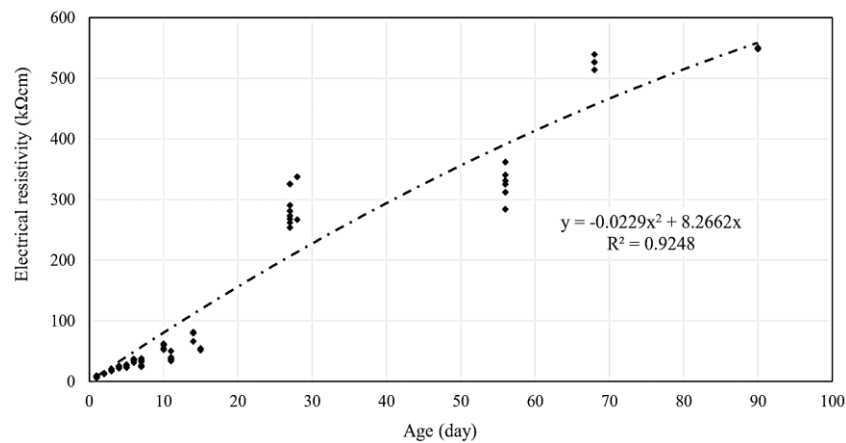

$y = -0.0229x^2 + 8.2662x$
$R^2 = 0.9248$

Figure 6. Electrical resistivity vs. age for water curing

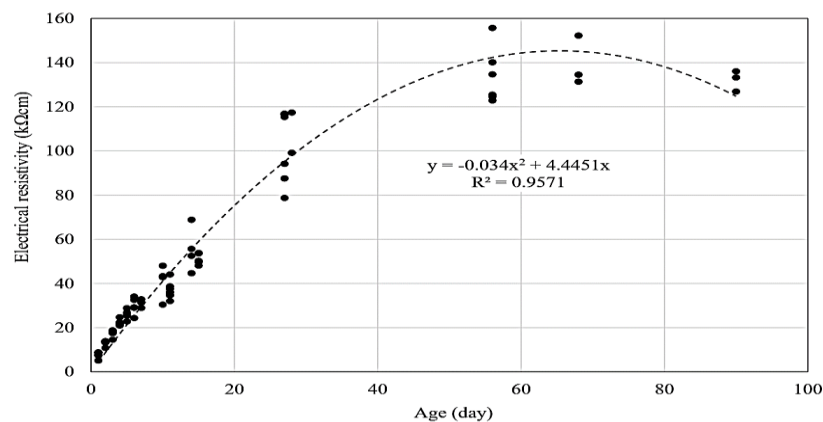$y = -0.034x^2 + 4.4451x$
$R^2 = 0.9571$

Figure 7. Electrical resistivity vs. age for sodium chloride solution curing
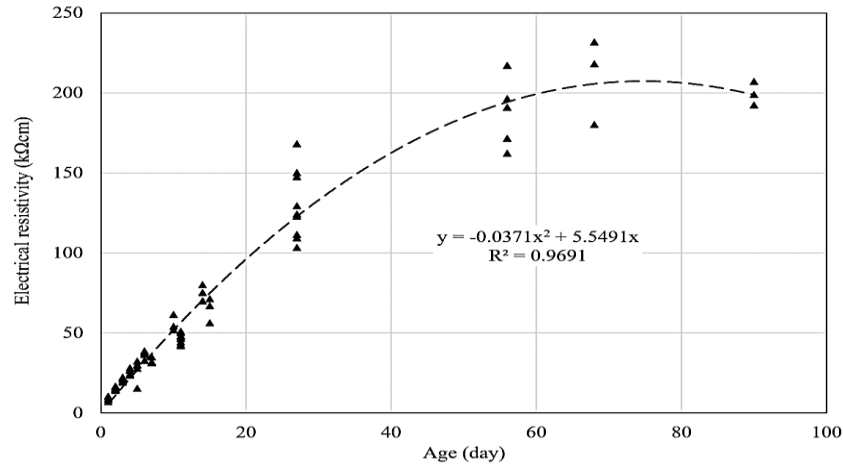
Figure 8. Electrical resistivity vs. age for magnesium sulphate solution curing

As shown, electrical resistivity increased by increasing the sample's age due to the hydration reaction, indicating a reduction in the ion concentration or composition of the mixes. Also, the hydration reaction by formation of a large number of hydration products, blockage of the ion's conductive paths, and a decrease in porosity, makes the concrete's microstructure much denser and causes ER to increase. Increase in ER vs age has been reported by many researchers [37, 46]. Further explanation is that micro silica reacts with calcium hydroxide and water and fills the capillary cavities by producing hydrated calcium silicate. Therefore, the connection between capillary pores is broken and the ions barely move inside concrete. On the other hand, the reduced concentration of OH^- ions as a result of these reactions sharply decreases the conductivity of the pore's fluid because [41] the electrical conductivity of OH^- is about three times greater than that of other dissolved ions in pore water, hence reducing its concentration, and this has a greater effect on increasing the ER. The low water/binder ratio used in UHPC construction also has a positive effect on its electrical resistivity, as it reduces the volume and connectivity of the porous network. Figure 9 shows all the three previous diagrams in one diagram for a better comparison of the increased slope of electrical resistivity under different curing conditions.
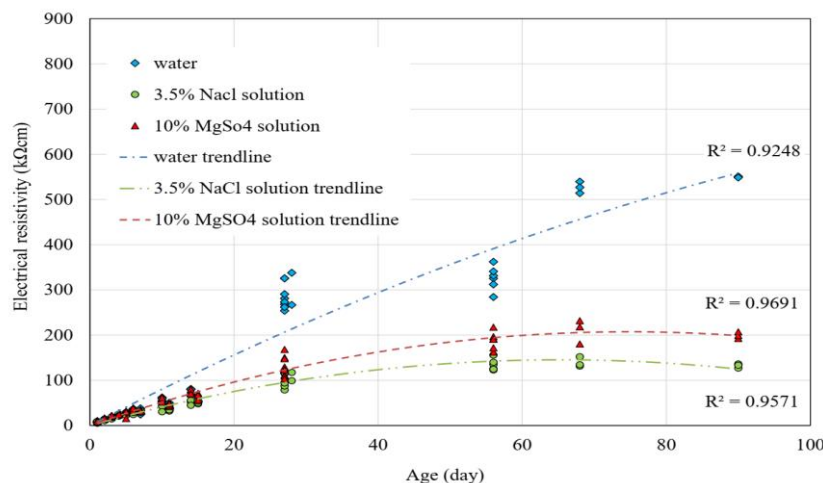
Figure 9. Comparison of the slope of electrical resistivity as a function of the specimens' age under different curing regimens

The comparison of the slope of increase in electrical resistivity under different curing conditions indicates that corrosive environments reduced it, relative to curing in water. It can be observed in Figure 7 that the increase rate trend lines, especially for chloride and sulphate solution, become stable after 56 days, approximately. Stable ER values after 98 days are also reported by Pyo et al. [31] for chloride-containing UHPC specimens. The most important factors affecting ER of concrete are the amount of concrete saturation, the amount and chemical composition of pore solution, chemical constituents of concrete, and the capillary pore structure and their connectivity in concrete. ER is also affected by temperature [15, 37]. In general, ions such as Al^{3+}, Ca^{2+}, Si^{4+} and K^- exist in the porous solution of concrete and ions types and their amounts significantly affect ER of concrete [22]. Any factor changing the concentrations of these ions in the pore solution such as cement substitutes, concrete carbonation, or penetration of any chemical solution from the curing environment can affect the electrical resistivity of concrete. According to Figure 9,

a sodium chloride solution is more effective than a magnesium sulphate one in reducing ER of UHPC. The condition of all samples was fully saturated at the time of testing. As the concrete structure becomes denser due to the continuation of the hydration reaction, the pore size and their connectivity are expected to decrease. According to what was concluded in the previous section about compressive strength, and also in the final section, which microstructure investigation will confirm, the number of pores and their connection in the sample cured in magnesium sulphate solution is more than those in sample cured in sodium chloride solution. Therefore, considering the further reduction of ER in samples cured in sodium chloride than that of those cured in magnesium sulphate solution, it can be concluded that over time, as the hydration reaction is completed, the role of pore solution conductivity will increase in determining electrical resistivity. This result is even more interesting when considering that the concentration of sodium chloride solution is much lower than that of magnesium sulphate solution. The variations

in mean ER of the samples under different environments are shown in Figure 10 for better comparison. The numbers on the columns represent the percentile changes in mean ER under corrosive environments compared to water.
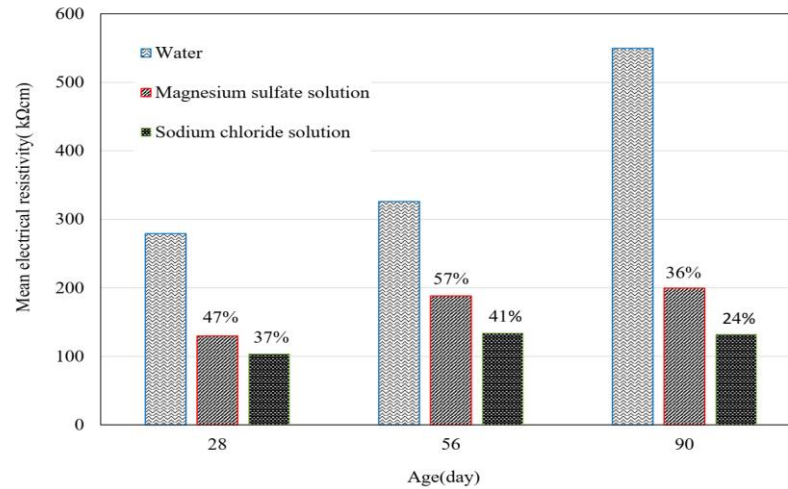
Average electrical resistivity under different curing regimens and percentile reduction relative to water

3.3. Relationship between compressive strength and electrical resistivity of the samples under different curing conditions

Compressive strength (CS) is an important mechanical property of concrete. Its increase contributes to the formation of more hydration products with time. At the same time, with the growth of hydration products in the pores, their connection is disconnected and ER increases. The interfacial transition zone (ITZ) strength plays a key role in determining the CS, but it does not affect ER. On the other hand, the chemical components of concrete's pore solution have no significant effect on CS, yet they strongly affect ER. Furthermore, the pore structure, including the volume of capillary pores and their interconnection, is crucial in determining the movement of ions in concrete. Therefore, the selection of

water/cement ratio has a great impact on ER [44]. The effect of water/cement ratio on CS has also been widely accepted as an incontrovertible fact. Therefore, it can be concluded that the relationship between ER and CS can be determined based on their relationship with the permeability of concrete. Both ER and CS present hydration features of cementitious materials with curing time [47]. The investigation of the microstructure in the following sections demonstrates and confirms that there is an intrinsic correlation between the ER and CS of concrete. Many researchers have conducted experimental research to find out the relationship between ER and CS of concrete [15, 47, 14, 26]. However, due to the influence of various factors such as constituents and mixing design on both ER and CS in each type of concrete, the relationship between them will be affected. Therefore, it is necessary to propose a suitable equation for UHPC. As presented in previous sections, the development curves of

CS and ER follow ascending trends over time.

Diagrams a, b, and c in Figure 11 show the relationship between mean ER and corresponding CS of UHPC samples at 7, 14, 28, 56 and 90 days for different curing conditions. For instance, the last point on the diagram associated with water curing conditions with an ER coordinate of 550 kΩ-

cm and a CS of 112 MPa was obtained from the mean ER and CS of 90-day similar samples. In Figures 9-a and 9-b, it is observed that CS becomes greater as ER increases. A relationship between ER and CS in water curing is proposed as a logarithmic positive equation, as Xu et al. [46] and de Medeiros-Junior et al. [14] did, even though not for UHPC.
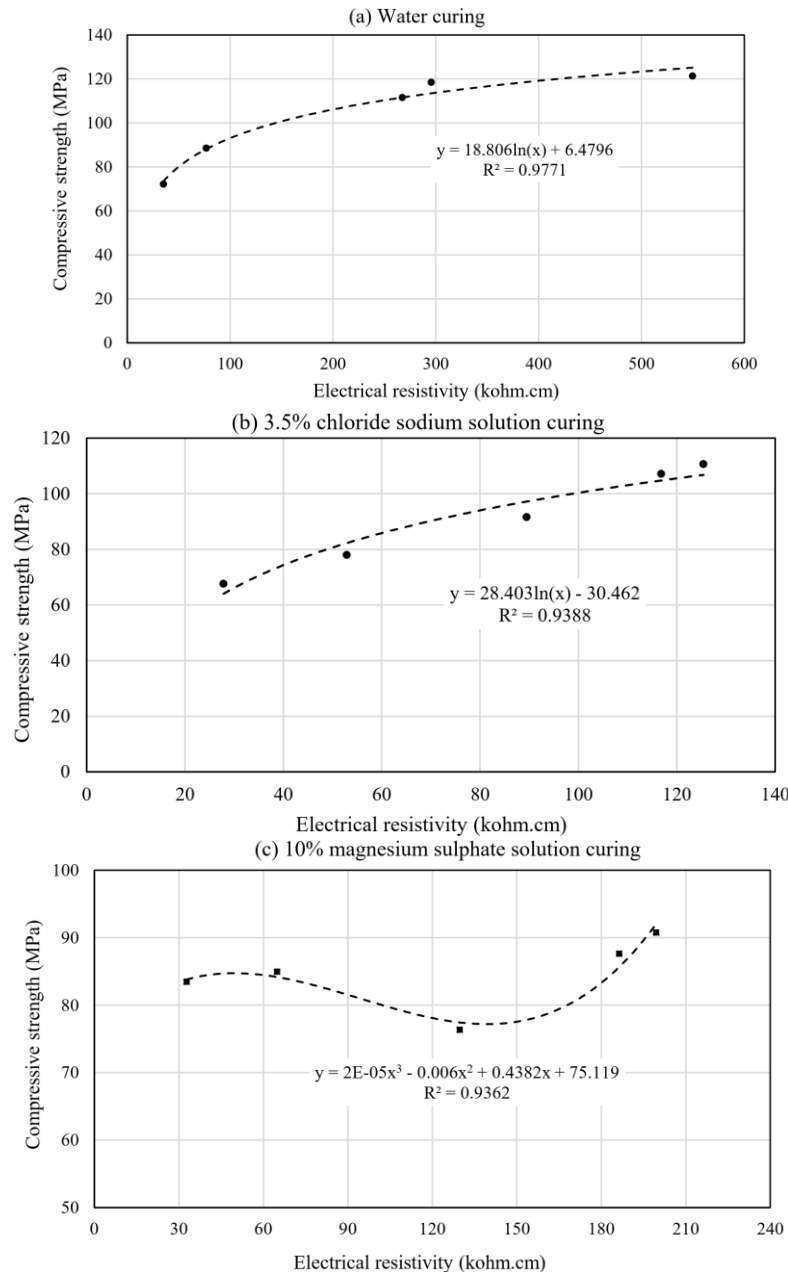

Figure 10.   Relationship between compressive strength and ER at standard ages for different curing regimens

A summary of experimental conditions and proposed equations of several studies is presented in Table 6.

Table 6. Review of experimental conditions and proposed equations in the literature

Ref.	Maximum compressive strength	Maximum electrical resistivity	Shape and size of the specimens	Electrical resistivity test method	Equation parameters	Example of the equations proposed in the reference	Units of equation's parameters
[14]	45.2	8.3	10×20mm Cylinder	Four-point probe technique (Wenner's method).	Compressive strength and corresponding electrical resistivity of concrete mixes with similar materials but different mixing design	$CS = 35.49\ln(ER) - 29.29$	kΩ.cm/MPa
[44]	89.94	85.28			Compressive strength and corresponding electrical resistivity of concrete mixes with similar materials but different mixing design	$CS = 14.71\ln(ER) + 16.86$	kΩ.cm/MPa
[45]	54.7	0.374 (24h)	Prism/ 40×40×160 mm	Non-contact/ bulk electrical resistivity	Compressive strength of the samples at 28 days and electrical resistivity at 24 h, for different mix design mortars	$CS_{28d} = 8.76ER_{24} + 20.41$	Ω.m/MPa
[37]	70	14.40	Cubic/ including unreinforced specimens and reinforced specimens. Unreinforced specimens cured in water and reinforced specimens in air	Four-point probe technique (Wenner's method).	Compressive strength and electrical resistivity for unreinforced and reinforced with Ø10, Ø14 or Ø20 reinforcement rebars of nine different mix designs	$CS = 57.2\ln(ER) - 84.3$	kΩ.cm/MPa
[15]	51.3	7.91	150 mm cubes/ 100 mm by 200 mm cylinders Water curing at 20 °C	Four-point probe technique (Wenner's method	Electrical resistivity and corresponding compressive strength at 1, 2, 4, 7, 14 and 28 days on 100 mm 200 mm cylinders for each mix design	$CS = 0.5654ER + 4.3608$	Ω.m/MPa

As presented in column 6 of Table 6, the proposed equations in many studies are derived from fitting curves to experimental data that relate to different mix designs or in which CS and ER do not necessarily correspond to each other. However, in the present study, ER and CS correspond to the same age. In addition, the measurement of ER is sensitive to various factors, such as the shape and size of the specimen, test method, and especially the degree of saturation and moisture content of concrete. Due to the lack of some researchers in reporting these factors during measurement in their research, it is not easy to compare the suggested relationships from the different studies. Figure 12 compares the proposed equation for water-cured specimens in this study with experimental data and proposed equations in several studies.
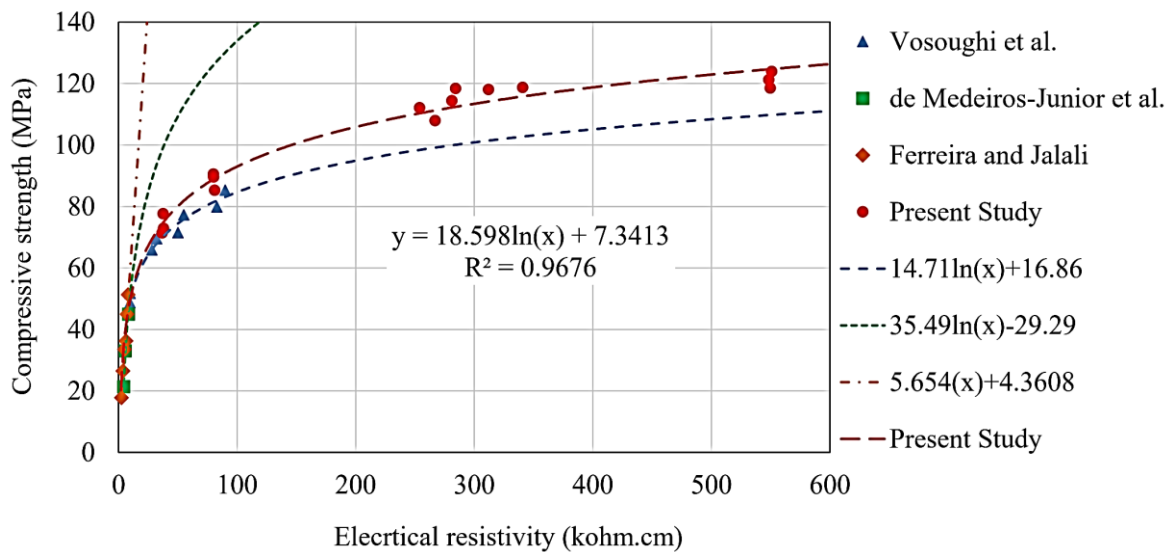

Figure 11. Comparison of proposed equation with results of several researches

Reviewing the proposed relationships of different researchers and comparing them in Figure 12 also shows that, due to differences in the constituent materials and mixing design, the use of the proposed relationships for ordinary concrete is not suitable for UHPC.

The equation, proposed by Vosoughi et al. [44] for concrete containing micro silica and natural filler up to the maximum CS and ER of the present experimental data, is used, up to 12.98% relative error is observed. On the contrary, the use of the now proposed equation fits well the experimental data in their study and the maximum relative error is only 6.29%.
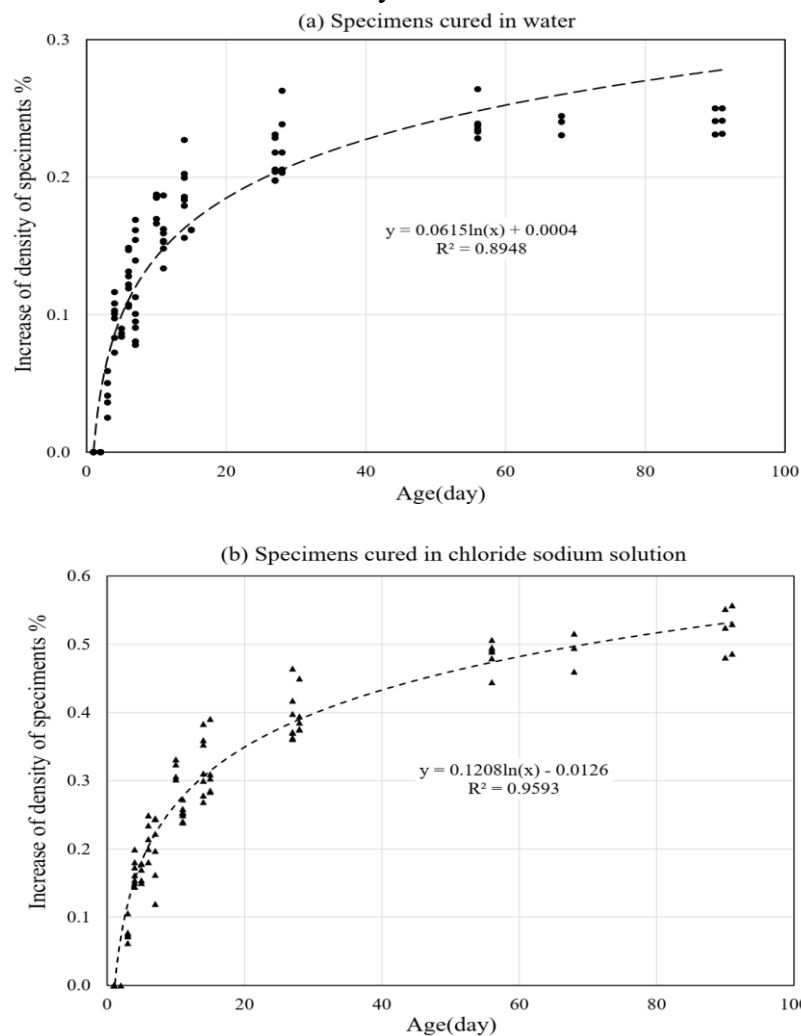
3.4. Analysis of the changes in density of the samples under different curing conditions

Figure 13 shows the percentage of density change (relative to day one) in samples cured under different environments and their relationship. It is shown that the rate of density gain was steeper at early ages, but, with the increase in the sample's age, the rate

slowed down because the hydration reaction continued in all curing environments, particularly at early ages, and the corrosive environments could not completely inhibit the reaction growth. The growth of hydration reaction and its products such as C-S-H (Calcium-Silicate-Hydrate) gels and ettringite increases the density of all samples over time by filling the pores and spaces between aggregates and the cement paste, and increasing the volume of the concrete solids [29]. A similar behaviour was noted by

Zhao et al. [50, 51] and Mangi et al. [25]. To better compare the density change process in different environments, Figure 14 shows a column chart of the percentages of density change in 9 samples over a 90-day period compared to the first-day density of the same sample. In Figures 11 and 12, the percentages of density change were obtained from difference between the sample's density at each age and the initial density divided by the initial density.
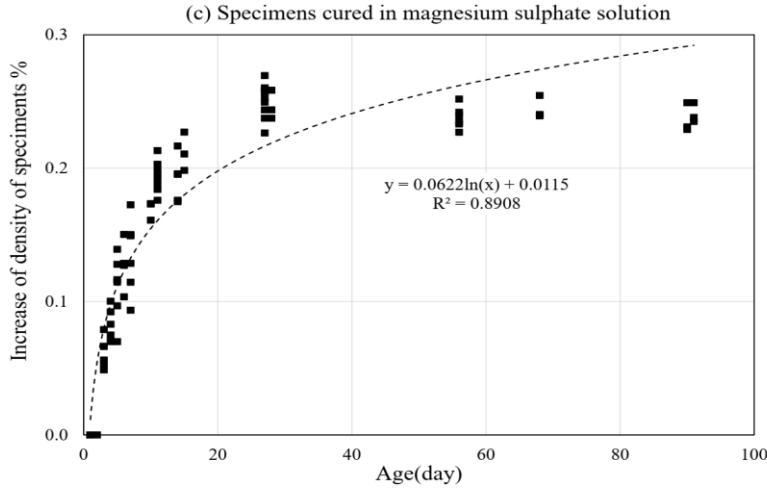

(a) Specimens cured in water

$$y = 0.0615\ln(x) + 0.0004$$
$$R^2 = 0.8948$$

(b) Specimens cured in chloride sodium solution

$$y = 0.1208\ln(x) - 0.0126$$
$$R^2 = 0.9593$$

Figure 12.   Relationship between density change and age under different curing regimens

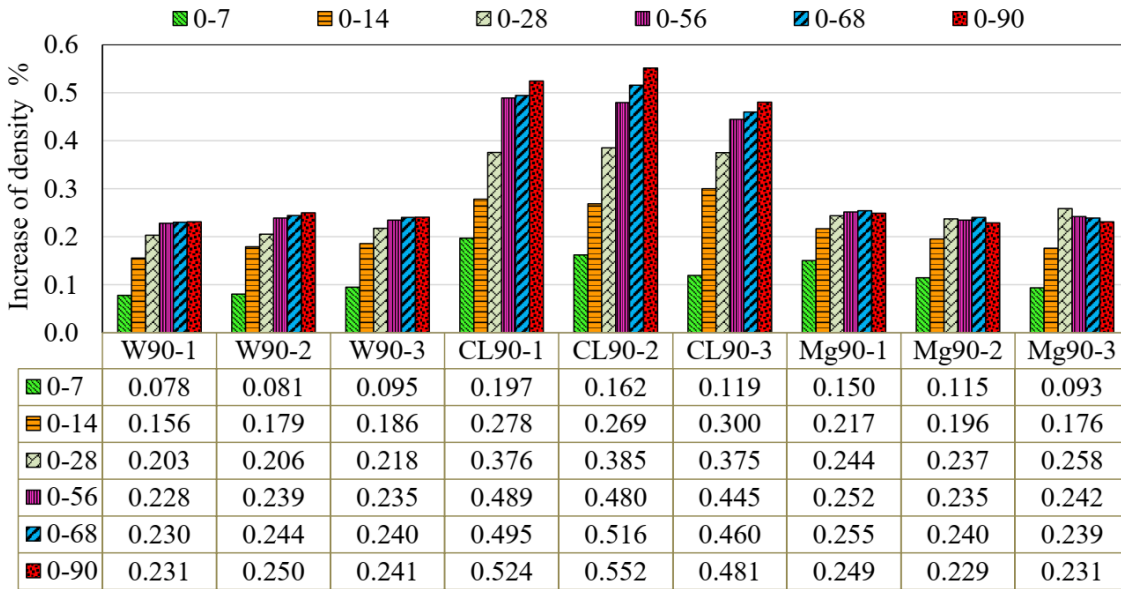|	W90-1	W90-2	W90-3	CL90-1	CL90-2	CL90-3	Mg90-1	Mg90-2	Mg90-3
0-7	0.078	0.081	0.095	0.197	0.162	0.119	0.150	0.115	0.093
0-14	0.156	0.179	0.186	0.278	0.269	0.300	0.217	0.196	0.176
0-28	0.203	0.206	0.218	0.376	0.385	0.375	0.244	0.237	0.258
0-56	0.228	0.239	0.235	0.489	0.480	0.445	0.252	0.235	0.242
0-68	0.230	0.244	0.240	0.495	0.516	0.460	0.255	0.240	0.239
0-90	0.231	0.250	0.241	0.524	0.552	0.481	0.249	0.229	0.231

Figure 13.   Percentile change in the density of specimens relative to their initial density under different curing regimens over the 90-day period

The analysis of the diagrams indicates that all samples experienced density gain with age. The density gain process will become slower and eventually almost nil when the hydration reactions in concrete are complete. Subsequently, the long-term exposure of concrete to corrosive conditions may result in the reaction of concrete structure with the corrosive agents. The final amount of density varies depending on the produced materials in the reaction. In other words, the formation of additional high-density hydration products in specimens exposed to corrosive environment is effective in increasing the sample's density. Since two effective factors on weight gain of concrete (the growth of C-S-H nanostructure and other cement gels and the growth rate of ettringite in the concrete

microstructure) are inversely related, in a condition where the optimal state is created in the formation of both structures, a higher density is seen in the specimens [5]. Also, deposition of salts dissolved in corrosive environments into the surface pores of the specimens increases the weight of the specimens. Recent condition is especially evident in specimens cured in sodium chloride (Figure 15).
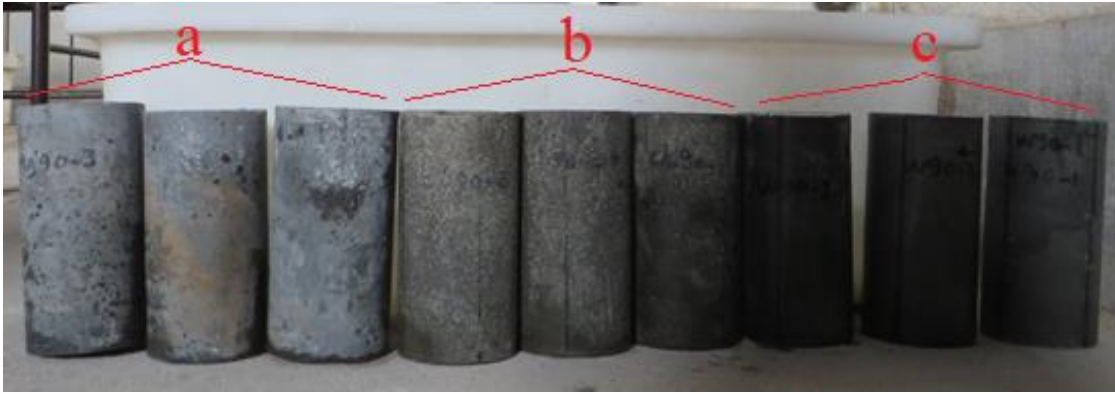

Figure 14.   Samples after 90 day curing: (a) three right samples in water, (b) three middle samples in sodium chloride solution, (c) three left samples in magnesium sulphate solution

The growth in density of the specimens immerged in 10% sulphate solution, in the early days up to 28 days, as the hydration reaction progresses, is slightly higher than that of the specimens cured in water. This behaviour is also reported by Zhoa et al. [51]. It is due to the formation of additional products such as ettringite and gypsum. A very slight decrease in density is observed in those specimens in the next days that indicates longer exposure can damage the surface of the specimens and cause spalling of damaged concrete and consequent reduction of weight. In Figure 15-c, minor damage to specimen's surface without cracking and remarkable spalling is visible, in parts of the sample surface by naked eye,

although it is a little difficult, and surface erosion is confirmed by feeling the surface's slight roughness, after 3 months. The results show that, despite high sulphate concentration and fast chemical attack, damage to UHPC after 3 months is relatively very low. This confirms the high durability of UHPC.

3.5. Evaluation of chloride ion penetration in samples under different curing conditions

Figure 16 shows the surface ER of some samples at 28 days. The AASHTO standard range in Table 1 is shown in dotted lines.
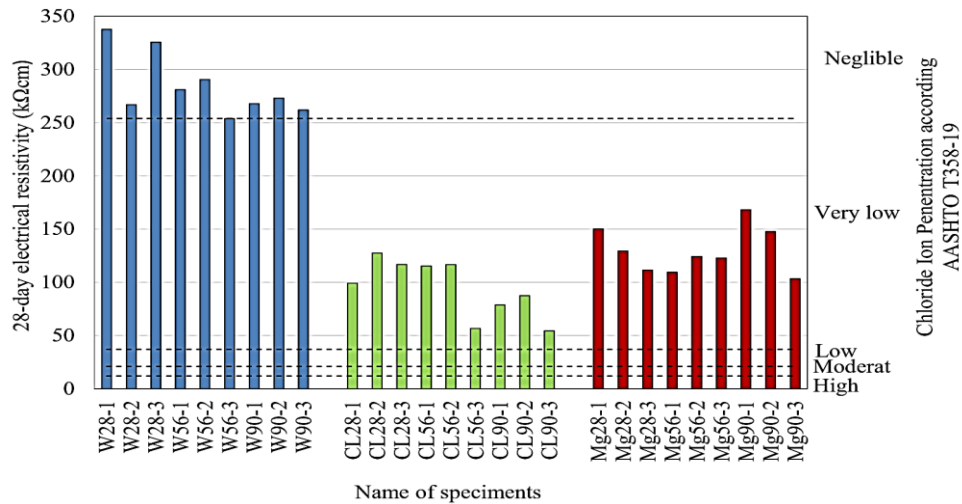
Figure 15. Determination of chloride ion penetration in specimens using electrical resistivity

3.6. Further discussion of results by examining the microstructure of concrete

As shown, the penetration rate of chloride ions was negligible in all water curing samples and the penetration rate was very low in samples cured with sodium chloride and magnesium sulphate solutions. This finding agrees with other evaluated methods. Mosavinejad et al. [28], by using ASTM C1202 on UHPC specimens under two curing regimes, conventional curing in a 20 ºC limewater tank and hot curing in a 70 ºC hot-water tank for 72 h, have detected negligible penetrability. Graybeal and Hartmann [16] also recorded the total charge passed at 28 days, according to ASTM C1202 and have reported negligible penetration rate for UHPC specimens under four curing regimes; steam (90 ºC, 95%RH), ambient air curing, lower temperature steam (60 ºC, 95%RH) and delayed steam curing until 15 days after casting.
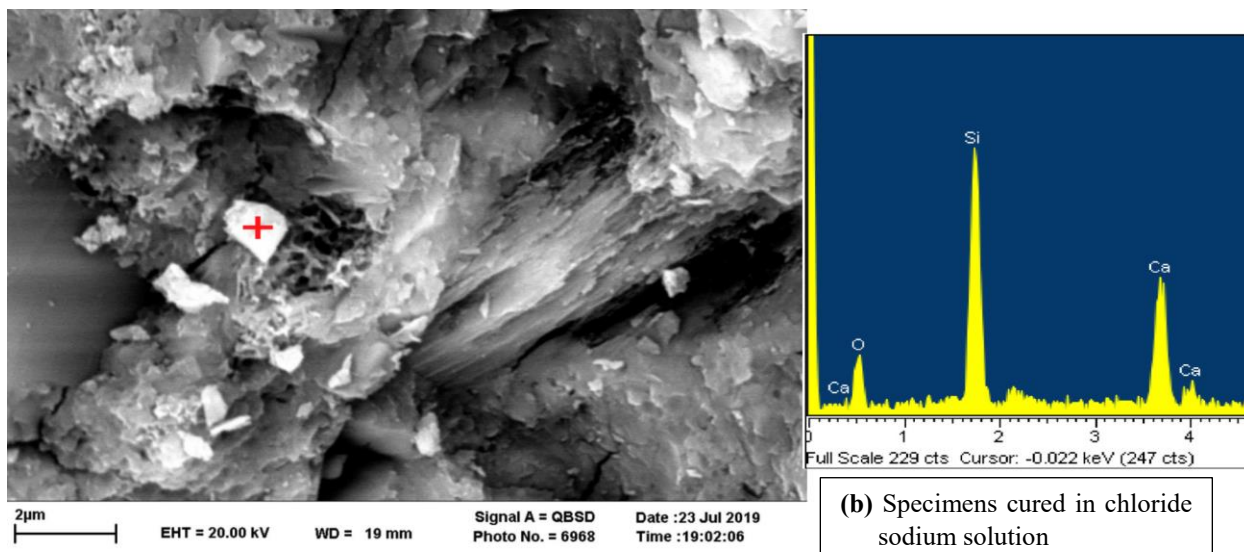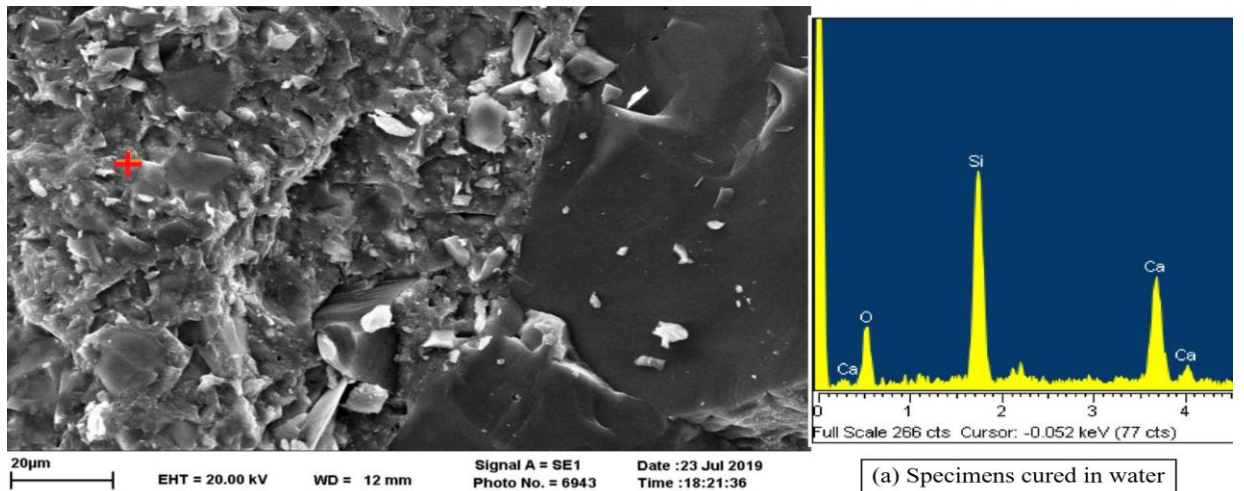
According to the results, UHPC is a great material for structures exposed to sulphate and chloride corrosive damage and that need to have a long service life.

The microstructure of concrete in contact with water and corrosive solutions of chloride and sulphate was studied via Scanning Electron Microscope (SEM) and Energy dispersive X-ray spectroscopy (EDS) for further explanation of the results obtained in the previous sections (Figure 16). To ensure from completing hydration process, these tests were conducted a long time after casting. Depending on size and position, there are four different types of pores in hardened concrete: interlayer pores, gel pores, capillary pores, and air cavities. The gel pores are thousands of times smaller than the capillary pores. Gel and interlayer pores are included in the occupied volume by the C-S-H strings. Capillary pores consist of a portion of concrete that is initially filled with water in fresh concrete rather than hydration products. Air cavities are further caused by inadequate packing and air confinement in concrete. The capillary pores are usually

maze- and tube-like, while air cavities are spherical and with larger sizes [32]. According to Power's report, the degree of permeability is mainly controlled by capillary porosity. The hydration reactions then break the connection between capillary pores and permeability is controlled by the gel pores. In concrete, the transition zone (the space between aggregates and cement paste) is the weakest part of the concrete due to the presence of pores and crystals of calcium hydroxide and ettringite. C-S-H gel is formed and the transition zone becomes nearly as dense as the matrix itself. Because of the low water to cement ratio in the manufacture of

UHPC and the pozzolanic reactions between calcium hydroxide and mineral impurities, the transition zone is stronger. The C-S-H structure is responsible for most engineering specifications of concrete, not only because it is a strong and stable phase, but also because it forms a continuous layer that agglomerates the main cement particles, forming a coherent texture. All other hydration products are discrete crystals that are inherently strong, yet unable to form strong bonds with the solid phases with which they are in contact; therefore, they cannot contribute much to the strength of concrete.
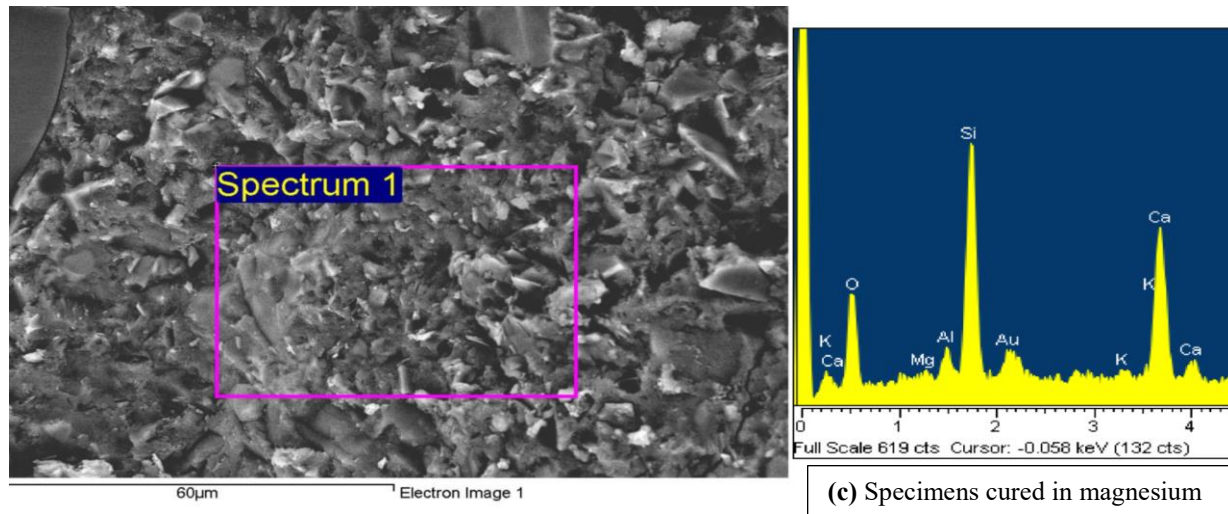

(a) Specimens cured in water

(b) Specimens cured in chloride sodium solution

(c) Specimens cured in magnesium

Figure 16. SEM images and EDS analysis of UHPC samples for different curing regimens

In the presence of water, chloride and sulphate ions enter the reactions and undesirable materials such as ettringite and gypsum are produced. This has adverse effects on the C-S-H gels and causes weakness in the transition zone, affecting the final properties of concrete. The thickness of the transition layer varies from 10 to 50 μm in concrete [32]. The present study on the microstructures of concrete in the transition zone confirmed the growth of hydration reactions in all three curing environments. Figure 16 shows a homogeneous and dense texture in all samples, which is the result of the growth of the hydration reaction and the formation of its products, especially the C-S-H structure that filling the spaces between aggregates and cement. The C-S-H in cement paste has a variable stoichiometry, for this "-" is laid among C, S, and H. In water-cured samples (Figure 16a), there are no specific connected pores or clear and obvious cracks at the aggregate boundary. Creating a dense gel improves CS and, on the other hand, increases the ER by disrupting the ion conduction pathway. Figure15b and 15c for samples cured in sodium chloride solution and magnesium sulphate solution show that, in addition to some small pores, cracks appear in the cement paste. It should be noted that, in the sulphate solution cured samples, the amount of connected pores, cracks and un-hydration products, is more than that of sodium chloride solution cured samples. Reducing the amount of C-S-H gel and the presence of connected pores decrease CS and ER. In addition, ACI201.2R-16 explains that the generation of ettringite and gypsum (Calcium sulphate dehydrate, $CaSO_42H_2O$) is the consequence of sulphate attack of concrete. The existence of ettringite increases the solid content of concrete, and causes expansion and cracking, and gypsum results in softening and loss of CS. When there is a sulphate attack by magnesium sulphate, brucite is produced, reacting with silica gel and causing destruction of the C-S-H gel structure [29]. In the EDS spectrum in Figure 16-c, the highest peak is related to Si. AL, Ca, K and Mg peaks are minor, related to hydrated products such as ettringite and calcium hydroxide. Small Mg peak confirms the very low penetration of magnesium into the product structure and can be cited as evidence for magnesium hydroxide (Brucite)

production. According to the literature, magnesium ions can delay the hydration process. This can explains the reason for the decrease in the difference in compressive strength with the control sample by increasing the age. This result is consistent with Roberti's research [36]. They also reported a decrease in the tendency to reduce strength from 1 day to 28 days due to the delayed effect of magnesium ions. Another SEM image in Figure 16-c shows the creation of very low needle-like ettringite crystals in the 90-day

sample in the vicinity of magnesium sulphate. In order to investigate further the influence of chloride ions on UHPC, the microstructure of two samples (taken from depth of 1-3 cm from the surface) was examined by X-ray diffraction (XRD) analysis and the results are shown in Figure 18. The first sample was exposed to a 3.5% sodium chloride solution for 28 days, and the second sample, following 28 days of curing in water, was exposed to a 3.5% sodium chloride solution for 350 days.
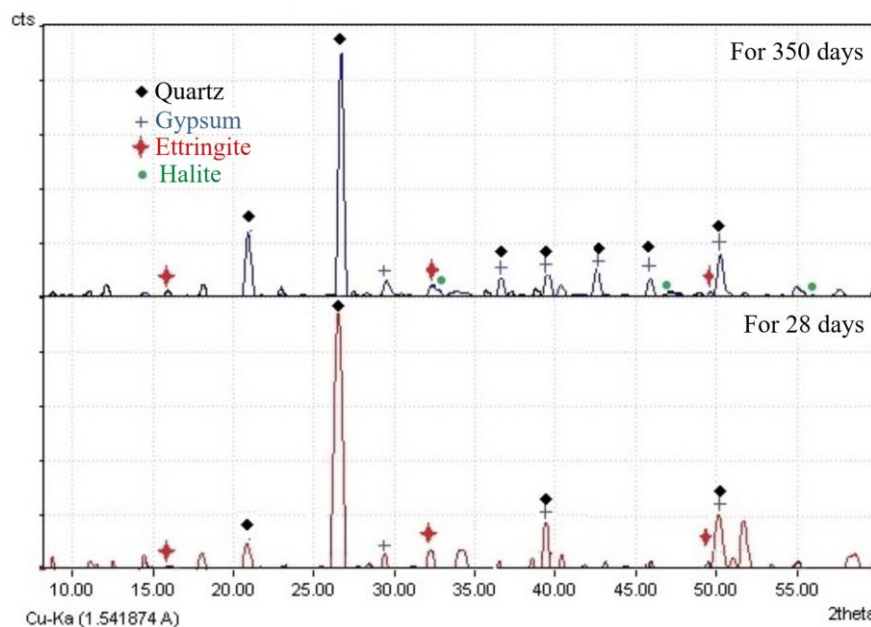

Figure 17. XRD analysis of UHPC samples cured in a chloride sodium solution

According to the results, there was no halite (mineral form of sodium chloride, NaCl) in the XRD spectrum of the first sample, implying that its amount was so low it could not be detected. In the second sample, the

amount of halite was about 1.3 wt% of the sample, which was very low regarding the exposure duration of the sample to the solution. Figure 19 shows the XRD analysis of samples exposed to corrosive solution and water for 90 days. Samples were taken from a depth of 1-3 cm from the surface.
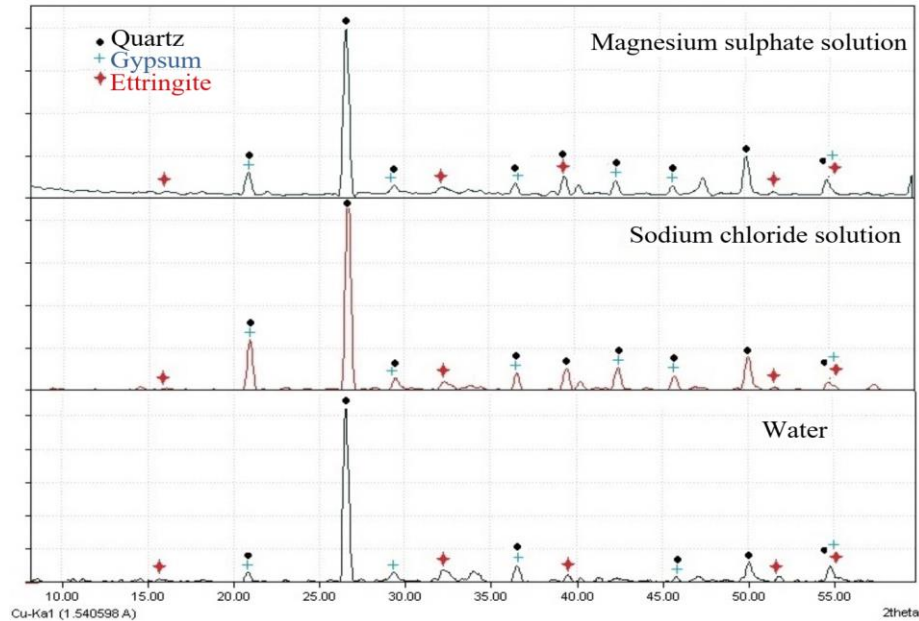
Figure 18. XRD analysis of UHPC samples exposed to corrosive solutions and water

As observed in Figure 19, the highest peak belongs to quartz, which is due to the presence of many siliceous compounds such as silica sand in the sample composition. This observation is compatible with the EDS spectrums presented in Figure 17. However, a review of the reports obtained from XRD analysis shows that the relative percentages of ettringite and gypsum in the sample taken from the specimen cured in magnesium sulphate is higher than the corresponding values in the specimens cured in sodium chloride and water, respectively. The amount of magnesium hydroxide detected was about 5.2% of the relative weight of this sample. This study justifies the results obtained in the previous sections.

In general, the results indicate the very low permeability of UHPC. Because of its high resistance to chloride ion penetration, this concrete further prevents corrosion of the structural rebars, a major problem in offshore structures. Therefore, it is an ideal material for use in those structures (e.g. bridge piers, docks, and oil platforms). Also, its durability along with its high strength properties decrease maintenance costs. On the other hand, it completely justifies the higher initial building cost of this concrete in comparison with the conventional concrete by allowing the use of smaller cross-section members, thereby reducing the dead load of the structure.

4. Conclusion

Given the tests and analyses, the findings can be summarized as follows:

- Corrosive environments delayed the increase in compressive strength of concrete, resulting in 8.73% and 25.50% reductions in chloride and sulphate environments, respectively, relative to that of the control samples at 90 days;

- The effect of sulphate environment on compressive strength was more destructive than that of the chloride environment;

- Electrical resistivity increased with age. The equations between ER and age were presented for UHPC in water, sulphate and chloride corrosive environments;

- The corrosive environments reduced the growth rate over time of ER compared to that of the control specimen. In this regard, the effect of sodium chloride solution was more than that of the magnesium sulphate solution;

- The electrical resistivity and compressive strength of samples were correlated due to the association of each characteristic with the porosity and permeability of concrete. The closest relationships with the results were presented to estimate the CS of concrete by ER in UHPC;

- Over time, the role of pore solution conductivity will increase in determining the electrical resistivity;

- The density of all samples increased with age. The amount of density in each sample depended on the types of final materials produced in the reactions and the effect of corrosive environments on the concrete surface. Equations of density of UHPC versus age in water and corrosive environments were presented;

- Curing in a corrosive environment negatively affects the final permeability of the specimens, but its destructive effect on UHPC is small. Chloride ions penetration rate was examined by surface ER according to AASHTO T358-19. The results indicated negligible penetration rates in the control samples, and very low penetration in the samples cured for 28 days in corrosive sulphate and chloride environments. Therefore, the UHPC performance in structure with long design service life is very satisfactory;

- The microstructure of UHPC according to electron microscopy studies indicated that main hydration product is C-S-H structures and corrosive environments were unable to destabilize significantly its structure.

- According to the examination of the microstructure of the samples in the vicinity of sodium chloride solution with X-ray diffraction spectrum, only about 1.3 wt% of the sample, halite penetrated into concrete, after 350 days of exposure to sodium chloride solution; however, there was no detectable halite penetration in a 28-day sample in the same condition.

REFERENCES

[1] AASHTO (2007). Standard method of test for electrical indication of concrete's ability to resist chloride ion penetration. AASHTO T277-07. Washington, DC., American

Association of State Highway and Transportation Officials.

[2] AASHTO (2014). Standard method of test for surface resistivity indication of concrete's ability to resist chloride ion penetration. AASHTO TP-95. Washington, DC, American Association of State Highway and Transportation Officials.

[3] AASHTO (2019). Standard method of test for surface resistivity indication of concrete's ability to resist chloride ion penetration. AASHTO T358-19. Washington, DC, American Association of State Highway and Transportation Officials.

[4] Aicha, M. B. (2020), The superplasticizer effect on the rheological and mechanical properties of self-compacting concrete, New Materials in Civil Engineering, Elsevier: 315-331.

[5] Amiri, M.,Tanideh, P. (2020). "Microstructural assessment of the effect of sulfate environments on the mechanical mroperties of moncrete." Modarres Civil Engineering 19(6): 1-14.

[6] Asadi Shamsabadi, E., Ghalehnovi, M., de Brito, J., et al. (2018). "Performance of concrete with waste granite powder: The effect of superplasticizers." Applied Sciences 8(10): 1808.

[7] ASTM (2013). Standard specification for chemical admixtures for use in producing flowing concrete. ASTM C1017M-13e1. West Conshohocken, PA, ASTM International.

[8] ASTM (2015). Standard specification for silica fume used in cementitious mixtures. ASTM C1240-15. West Conshohocken, PA, ASTM International.

[9] ASTM (2017). Standard specification for chemical admixtures for concrete. ASTM C494M-17. West Conshohocken, PA, ASTM International.

[10] ASTM (2018). Standard test method for compressive strength of cylindrical concrete specimens. ASTM C39M-18. West Conshohocken, PA, ASTM International.

[11] Azarsa, P.,Gupta, R. (2017). "Electrical resistivity of concrete for durability evaluation: A review." Advances in Materials Science and Engineering 2017: 1-30.

[12] Büyüköztürk, O.,Taşdemir, M. A. (2012), Nondestructive testing of materials and structures, Springer Science & Business Media.

[13] Chen, Y., Yu, R., Wang, X., et al. (2018). "Evaluation and optimization of Ultra-High Performance Concrete (UHPC) subjected to harsh ocean environment: Towards an application of Layered Double Hydroxides (LDHs)." Construction and Building Materials 177: 51-62.

[14] de Medeiros-Junior, R. A., da Silva Munhoz, G.,de Medeiros, M. H. F. (2019). "Correlations between water absorption, electrical resistivity and compressive strength of concrete with different contents of pozzolan." Revista ALCONPAT 9(2): 152-166.

[15] Ferreira, R. M.,Jalali, S. (2010). "NDT measurements for the prediction of 28-day compressive strength." NDT & E International 43(2): 55-61.

[16] Graybeal, B. A.,Hartmann, J. L. (2003). Strength and durability of ultra-high performance concrete. Concrete Bridge Conference.

[17] Hornbostel, K., Larsen, C. K.,Geiker, M. R. (2013). "Relationship between concrete resistivity and corrosion rate–a literature review." Cement and Concrete Composites 39: 60-72.

[18] http://www.sharghcement.ir/index.php?pgrec=produce_type2.

[19] Joshaghani, A.,Moeini, M. A. (2018). "Evaluating the effects of sugarcane-bagasse ash and rice-husk ash on the mechanical and durability properties of mortar." Journal of Materials in Civil Engineering 30(7): 04018144.

[20] Khaksefidi, S.,Ghalehnovi, M. (2020). "Effect of reinforcement type on the tension stiffening model of Ultra-High Performance Concrete (UHPC)." Journal of Rehabilitation in Civil Engineering 8(3): 72-86.

[21] Khaksefidi, S., Ghalehnovi, M.,De Brito, J. (2021). "Bond behaviour of high-strength steel rebars in normal (NSC) and ultra-high performance concrete (UHPC)." Journal of Building Engineering 33: 101592.

[22] Khanzadi, M., Tadayon, M., Maleki, M. S., et al. (2017). " Measuring the electrical resistivity of concrete by bulk, surface, galvapulse and the electrical conductivity methods." Concrete Research Journal 10(3): 19-28.

[23] Langeroudi, M. A. M.,Mohammadi, Y. (2018). "The effects of nanoclay on rheological, mechanical and durability properties of cement composites." concrete research journal 11(1): 61-74.

[24] Madani, H.,Pourjhanshahi, A. (2018). "An investigation on the pozzolanic reactivity of different materials and their effects on the properties of Ultra-High Performance Concrete (UHPC)." Amirkabir Journal of Civil Engineering 50(4): 707-724.

[25] Mangi, S. A., Ibrahim, M. H. W., Jamaluddin, N., et al. (2019). "Short-term effects of sulphate and chloride on the concrete containing coal bottom ash as supplementary cementitious material." Engineering Science and Technology, an International Journal 22(2): 515-522.

[26] Medeiros-Junior, R. A., Gans, P. S., Pereira, E., et al. (2019). "Electrical resistivity of concrete exposed to chlorides and sulfates." ACI Materials Journal 116(3).

[27] Mehrinejad Khotbehsara, M., Mohseni, E., Ozbakkaloglu, T., et al. (2017). "Durability characteristics of self-compacting concrete incorporating pumice and metakaolin." Journal of Materials in Civil Engineering 29(11): 040172181-040172189.

[28] Mosavinejad, S. G., Langaroudi, M. A. M., Barandoust, J., et al. (2020). "Electrical and microstructural analysis of UHPC containing short PVA fibers." Construction and Building Materials 235: 117448.

[29] Oneill, R., Hill, R. L., Butler, W. B., et al. (2016). "Guide to durable concrete." ACI201 2: 2-5.

[30] Polder, R. B. (2001). "Test methods for on site measurement of resistivity of concrete—A RILEM TC-154 technical recommendation." Construction and building materials 15(2-3): 125-131.

[31] Pyo, S., Tafesse, M., Kim, H., et al. (2017). "Effect of chloride content on mechanical properties of ultra high performance concrete." Cement and Concrete Composites 84: 175-187.

[32] Rafiee, A. (2012), Computer modeling and investigation on the steel corrosion in cracked ultra high performance concrete, kassel university press GmbH.

[33] Rahdar, H. A.,Ghalehnovi, M. (2016). "The characteristic of ultra-high performance concrete and cracking behavior of reinforced concrete tensile specimens." Journal of Structural and Construction Engineering 3(2): 42-58.

[34] Rahdar, H. A.,Ghalehnovi, M. (2016). "Post-cracking behavior of UHPC on the concrete members reinforced by steel rebar." Computers and Concrete 18(1): 139-154.

[35] Ramezanianpour, A. A., Zolfagharnasab, A., Bahmanzadeh, F., et al. (2018). " Assessment of high performance concrete containing mineral admixtures under sulfuric acid attack." Amirkabir Journal of Civil Engineering 50(1): 121-138.

[36] Roberti, F., Cesari, V. F., de Matos, P. R., et al. (2020). "High-and ultra-high-performance concrete produced with sulfate-resisting cement and steel microfiber: Autogenous shrinkage, fresh-state, mechanical properties and microstructure characterization." Construction and Building Materials: 121092.

[37] Sabbağ, N.,Uyanık, O. (2018). "Determination of the reinforced concrete strength by apparent resistivity depending on the curing conditions." Journal of Applied Geophysics 155: 13-25.

[38] Saeidiyan, P., Madhkhan, M. (2016). Investigation durability of ultra high-strength concrete, reinforced with glass fibers under ice and melting cycles. 3rd National & 1st International Conference on Applied Researches in Civil Engineering,

Architecture & Urban Planning. Tehran, Iran.

[39] Sharbatdar, M. K.,Habibi, A. (2018). "Experimental evaluation of mechanical characteristics and durability of concrete specimens under combination of chloride-sulfate environment conditions and sulfate aggregate." Concrete Research Journal 10(4): 19-33.

[40] Shen, P., Lu, L., He, Y., et al. (2019). "The effect of curing regimes on the mechanical properties, nano-mechanical properties and microstructure of ultra-high performance concrete." Cement and Concrete Research 118: 1-13.

[41] Snyder, K. A., Feng, X., Keen, B., et al. (2003). "Estimating the electrical conductivity of cement paste pore solutions from OH−, K+ and Na+ concentrations." Cement and Concrete Research 33(6): 793-798.

[42] Spragg, R., Villani, C., Snyder, K., et al. (2013). "Factors that influence electrical resistivity measurements in cementitious systems." Transportation Research Record 2342(1): 90-98.

[43] Vakili, S.,Vakili, M. (2012), Concrete (strength, durability, corrosion) Fadak Isatis Publications Tehran.

[44] Vosoughi, P., Faezizadeh, S. F., Feizbakhsh, S., et al. (2015). "An Investigation of the possibility of estimating the compressive strength of concrete by using its' electrical resistance." Cumhuriyet Science Journal 36(4).

[45] Wei, X., Xiao, L.,Li, Z. (2012). "Prediction of standard compressive strength of cement by the electrical resistivity measurement." Construction and Building Materials 31: 341-346.

[46] Xu, W., Tian, X.,Cao, P. (2018). "Assessment of hydration process and mechanical properties of cemented paste backfill by electrical resistivity measurement." Nondestructive Testing and Evaluation 33(2): 198-212.

[47] Xu, W., Tian, X.,Wan, C. (2018). "Prediction of mechanical performance of cemented paste backfill by the electrical

resistivity measurement." Journal of Testing and Evaluation 46(6): 2450-2458.

[48] Yazıcı, H., Deniz, E.,Baradan, B. (2013). "The effect of autoclave pressure, temperature and duration time on mechanical properties of reactive powder concrete." Construction and Building Materials 42: 53-63.

[49] Zega, C. J., Santillán, L. R., Sosa, M. E., et al. (2020). "Durable performance of recycled aggregate concrete in aggressive environments." Journal of Materials in Civil Engineering 32(7): 03120002.

[50] Zhao, G., Li, J.,Shao, W. (2018). "Effect of mixed chlorides on the degradation and sulfate diffusion of cast-in-situ concrete due to sulfate attack." Construction and Building Materials 181: 49-58.

[51] Zhao, G., Li, J., Shi, M., et al. (2020). "Degradation of cast-in-situ concrete subjected to sulphate-chloride combined attack." Construction and Building Materials 241: 117995.